

Supporting Evidence for a 9.6 ± 1 ka Rock Fall Originating from Glacier Point in Yosemite Valley, California



SHAUN E. CORDES

*Department of Geology, Humboldt State University, 1 Harpst Street,
Arcata, CA 95521*

GREG M. STOCK

*National Park Service, Yosemite National Park, 5083 Foresta Road,
P.O. Box 700, El Portal, CA 95318*

BRANDON E. SCHWAB

*Department of Geology, Humboldt State University, 1 Harpst Street,
Arcata, CA 95521*

ALLEN F. GLAZNER

*Department of Geological Sciences, CB# 3315, University of North Carolina,
Chapel Hill, NC 27599-3315*

Key Terms: *Geological Processes, Geomorphology, Geochemistry, Rock Fall, Remote Sensing, Yosemite*

ABSTRACT

Large boulders exceeding 10 m^3 in exposed volume are widely scattered throughout Upper Pines Campground in eastern Yosemite Valley, Yosemite National Park, California. These enigmatic boulders rest up to 330 m from the base of adjacent talus slopes but lack geomorphic expressions typical of other large rock fall, debris flow, or glacial deposits in Yosemite. We evaluated four hypotheses for boulder deposition: (1) glacial deposition during ice retreat 15–17 ka, (2) fluvial deposition during a high-discharge flood event, (3) debris flow deposition, and (4) rock fall deposition. We utilized field mapping, spatial analysis, cosmogenic ^{10}Be exposure dating, and X-ray fluorescence analysis to investigate possible modes of deposition. A mean boulder exposure age of 9.6 ± 1 ka considerably post-dates glacial retreat from Yosemite Valley, effectively ruling out glacial deposition. Discharge and bed stress calculations indicate that although flooding could have been capable of entraining boulders at confined upstream locations, it is unlikely to have transported boulders as far as the Upper Pines area. Slope comparisons and evaluation of surface morphology of debris flow fans in Yosemite Valley suggest that the boulders did not result from debris flows. Geochemical

results identify a majority of boulders in Upper Pines as granodiorite of Glacier Point, corresponding to bedrock samples located at the summit of Glacier Point. We interpret boulders in Upper Pines Campground to result from a single large rock fall event originating from the east face of Glacier Point circa 9.6 ± 1 ka; they were subsequently partially buried by alluvial fan aggradation, modifying the original geomorphic expression.

INTRODUCTION

Located in the central portion of the Sierra Nevada, Yosemite Valley in Yosemite National Park, California, is a 1-km-deep glacially carved valley dominated by Late Cretaceous granitic plutons (Bateman, 1992) that have experienced multiple episodes of Pleistocene glacial erosion (Figure 1; Matthes, 1930; Huber, 1987). The Last Glacial Maximum (LGM) in the Sierra Nevada occurred circa 18–20 ka (Birkeland and Burke, 1988; Bursik and Gillespie, 1993; Phillips et al., 2009; and Rood et al., 2011), with recessional moraines documenting the subsequent retreat of ice from Yosemite Valley (Matthes, 1930; Huber et al., 1987). Glaciation presumably left the floor of the valley free of rock fall debris (Wieczorek and Jäger, 1996). Since the LGM, accumulations of boulders and other rock debris have created extensive talus fields and alluvial and debris flow fans on the valley floor beneath the cliffs. More than 925 rock falls and other slope

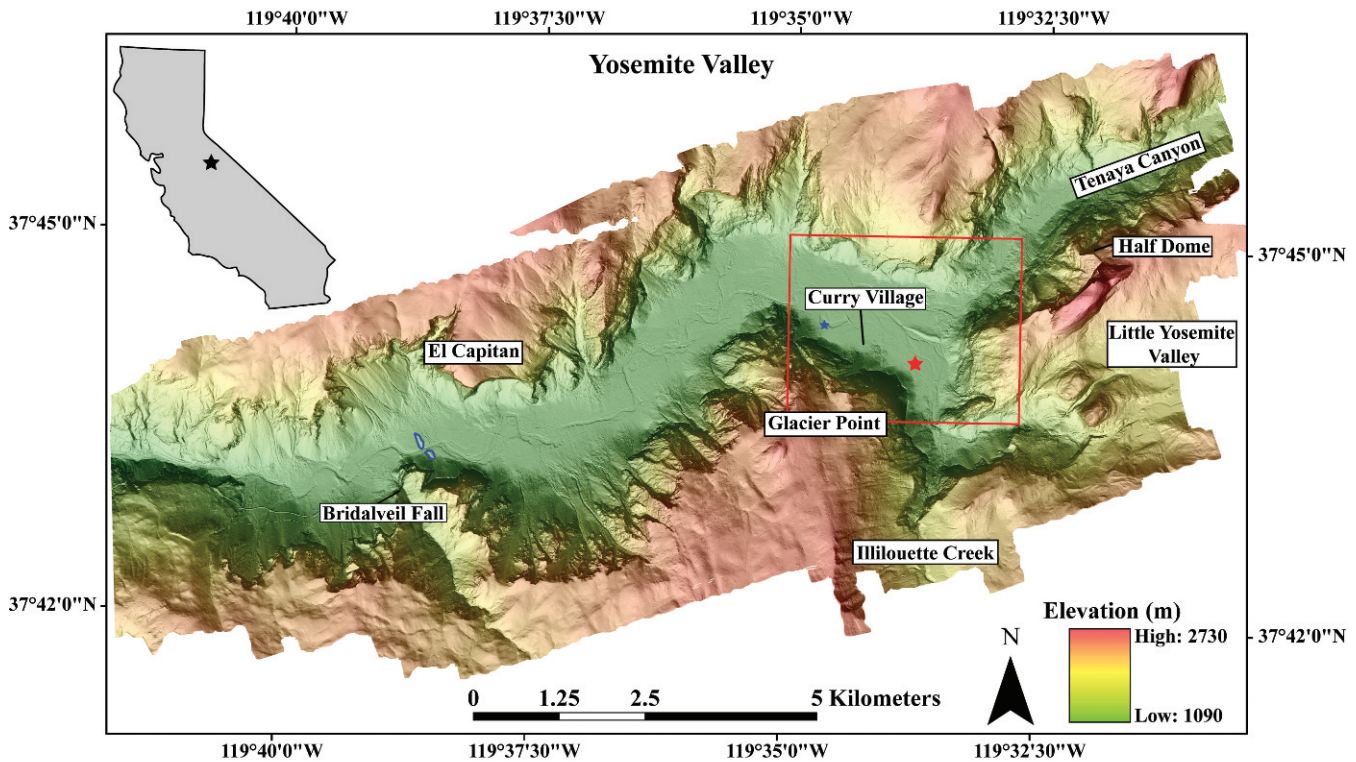


Figure 1. Shaded relief map of Yosemite Valley produced from a 1 m LiDAR-based digital elevation model (DEM). Red box indicates the field area, with the red star showing the location of Upper Pines Campground. The El Capitan recessional moraine responsible for damming the Yosemite Valley after the Last Glacial Maximum ice retreat is highlighted in blue. The blue star indicates the location of radiocarbon samples collected from a cutbank of the Merced River.

movements have been documented in Yosemite National Park since A.D. 1857, with most rock falls originating from the glacially steepened walls of Yosemite Valley (Stock et al., 2013). Features of particular interest are large boulder deposits (up to several million cubic meters in volume) with low surface slope angles that extend far beyond the base of talus slopes. These deposits are interpreted to represent extremely large and energetic rock falls, referred to in this setting as rock avalanches (Wieczorek et al., 1999; Stock and Uhrhammer, 2010).

A widely scattered group of boulders at the site of the Upper Pines Campground in eastern Yosemite Valley may represent one of these extremely large rock falls (Figure 2). However, these enigmatic boulders lack geomorphic expressions typical of other extremely large rock fall deposits (e.g., a continuous high density of angular boulders beyond the base of active talus, hummocky topography, and a back-sloping distal edge; Stock and Uhrhammer, 2010) (Figure 3). This raises the possibility that the boulders may instead have resulted from other depositional processes. Wieczorek et al. (1999) mapped these boulders as a debris flow deposit, but here again the morphology of the deposit is unlike those of other known debris flow deposits in Yosemite Valley.

Assessment of the hazard posed to Upper Pines Campground by rock falls is dependent on whether these boulders originated from rock falls or from some other processes. To address this question, we tested the following possible hypotheses for the origin of the boulders in Upper Pines Campground: (1) glacial deposition during retreat of the LGM glacier from Yosemite Valley, (2) fluvial deposition during one or more high-discharge flood events, (3) debris flow deposition, and (4) a large and energetic rock fall from the adjacent cliffs. We tested these hypotheses by mapping the boulders, analyzing the spatial distribution of boulders and boulder metrics, dating boulder exposure ages with cosmogenic nuclides, calculating potential paleo-discharge and bed stress conditions, and determining the composition of boulders and potential rock fall source areas on the adjacent cliffs.

GEOLOGIC SETTING

Lithologic Units and Field Relationships

The three lithologic units relevant to the study area are the granodiorite of Glacier Point, Half Dome



Figure 2. Upper Pines Campground boulder deposit and alluvial fan surface: (a) Boulder UPC-1, yielding an exposure age of 10.23 ± 0.23 ka and exposed height of 3.5 m; (b) Note the inset appearance of boulders on the fan surface; (c) Boulder UPC-4, with an exposure age of 5.7 ± 0.1 ka; (d) Boulder UPC-5, with an exposure age of 8.9 ± 0.8 ka and 1.4 m in exposed height. See Figures 3 and 5 for photo locations.

Granodiorite, and Cathedral Peak Granodiorite (Bateman et al., 1983; Peck, 2002; and Coleman et al., 2004). The summit ridge of Glacier Point above and west of Upper Pines Campground is composed of granodiorite of Glacier Point, with a marginal contact between the granodiorite of Glacier Point and Half Dome Granodiorite located approximately 500 vertical meters above the valley floor on the eastern face of Glacier Point; this contact diagonally crosses the northern face of Glacier Point and intercepts the valley floor west of Curry Village near Le Conte Memorial (Figure 4; Peck, 2002). The granodiorite of Glacier Point contains 15–25 percent anhedral mafic minerals that have a weak foliation, whereas the Half Dome Granodiorite contains 8–12 percent (Peck, 2002) mafic minerals, a weak to absent foliation, and euhedral hornblende phenocrysts 1–2 cm in length. The majority of eastern Yosemite Valley is composed of Half Dome Granodiorite, which is exposed for

another ~15 km east of Upper Pines Campground up the Merced River drainage to a marginal contact with Cathedral Peak Granodiorite near Merced Lake (Peck, 1980; Bateman et al., 1983; and Huber et al., 1989). Cathedral Peak Granodiorite is readily distinguishable from the other units due to its conspicuous blocky potassium feldspar megacrysts (Bateman et al., 1983).

Half Dome Granodiorite comprises the bedrock adjacent to Upper Pines Campground and the bedrock upstream of the campground, and could thus be found in glacial, rock fall, and fluvial deposits within the study area. Because the contact between Half Dome Granodiorite and Cathedral Peak Granodiorite is ~15 km up valley and east from Upper Pines Campground, large (generally >1 m³) boulders of Cathedral Peak Granodiorite could be found in glacial deposits (as seen within Yosemite Valley glacial moraines; Huber, 1987), and possibly, also in

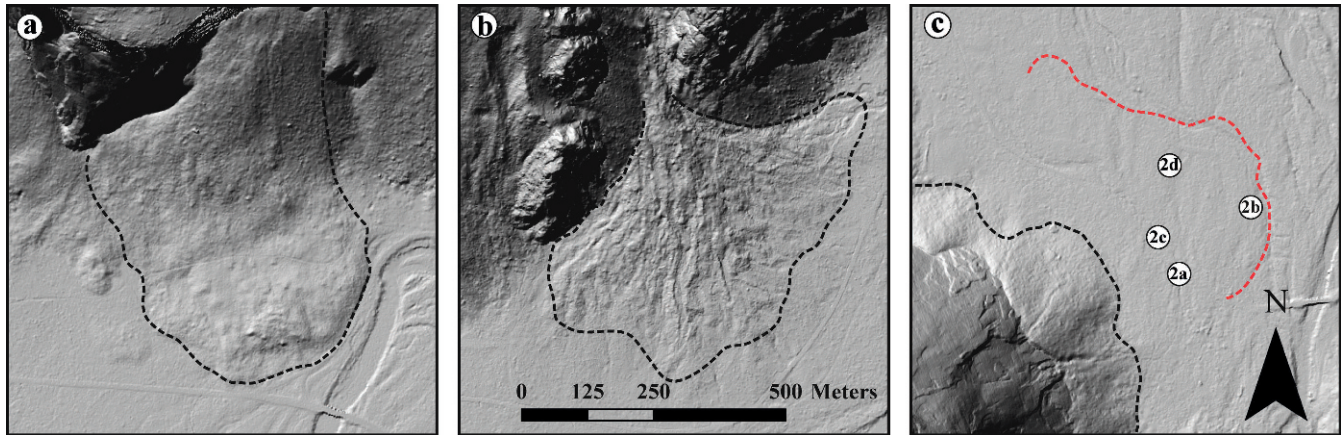


Figure 3. Morphology of rock avalanche, debris flow, and isolated boulder deposits in Yosemite Valley. (a) El Capitan Meadow rock avalanche: Note the distinct distal edge and hummocky topography. (b) Eagle Creek debris flow fan: Note the well-defined debris fan extruding out into Yosemite Valley and rough channelized surface. (c) Upper Pines Campground boulders: Note the lack of resolvable topography on the fan surface. Red dashed line shows the extent of large ($>1 \text{ m}^3$) boulders; black dashed line identifies the edge of the active talus slope beneath Glacier Point. Numbers and letters refer to boulder photo locations shown in Figure 2.

fluvial deposits as smaller cobbles and boulders (generally $<1 \text{ m}^3$).

A fourth sub-unit consisting of a leucocratic facies of Half Dome Granodiorite is also found within the field area. This sub-unit is part of a mafic-felsic lithologic cycle mapped in the Half Dome Granodiorite in several locations west of Tenaya Lake by Coleman et al. (2012). It consists of an eastern mafic margin that grades westward to a leucocratic top that forms a sharp western contact with the mafic margin of the next cycle. The leucocratic zones are generally thin and discontinuous bodies that appear sub-parallel to the outer contact of the Half Dome Granodiorite, occur along the outer and older margins of the pluton, and fade out towards the younger, interior contact with Cathedral Peak Granodiorite (Coleman et al., 2012). Leucocratic zones are characterized by high SiO_2 (72–78 weight percent), low MgO (<0.5 weight percent), and few mafic minerals, although they retain the euhedral hornblende phenocrysts that characterize the Half Dome Granodiorite (Coleman et al., 2012). Kistler (1973) mapped several of these leucocratic zones as aplites.

Glacial History of Yosemite Valley

Glacial ice has occupied Yosemite Valley on several occasions throughout the Pleistocene, with the earliest advances overtopping the valley walls and the youngest only partially filling the valley (Matthes, 1930; Wahrhaftig, 1962; and Huber, 1987). In Yosemite Valley, the LGM glacier is thought to have terminated west of Bridalveil Fall (Figure 1; Huber, 1987). In the Sierra Nevada, the LGM occurred

between 28 and 14.5 ka (Bursik and Gillespie, 1993; Phillips et al., 2009) and most likely began retreating at about 18 ka (Rood et al., 2011). Although the exact timing of deglaciation is unknown for Yosemite Valley, the valley is generally considered to have been free of ice by circa 15–17 ka (Huber, 1987; Wieczorek and Jäger, 1996).

Matthes (1930) and Huber and Snyder (2007) purport that the prominent recessional moraine near El Capitan was responsible for damming melting ice water and creating a shallow lake (Figure 1). As ice fully retreated out of Yosemite Valley, alluvial sedimentation advanced a delta westward, eventually infilling the lake and creating a flat valley floor at $\sim 1210 \text{ m}$ elevation above mean sea level (Matthes, 1930). Post-glacial breaching of the El Capitan moraine caused the Merced River to incise, preserving alluvial terraces on the periphery of the valley. Although most of the sediments in Yosemite Valley are relatively fine grained (sand and gravel), at the eastern end of Yosemite Valley near Happy Isles, the pronounced downstream decrease in the gradient of the Merced River has led to deposition of coarser debris on an alluvial fan in the vicinity of Upper Pines Campground (Figure 4).

METHODS

Field Mapping, Remote Sensing, and Spatial Analysis

We mapped 519 boulders by hand and global positioning systems (GPS) throughout the Upper Pines Campground. Our criteria for mapping boulders consisted of visually identifying boulders with estimated exposed volumes of $>1 \text{ m}^3$ and those inset

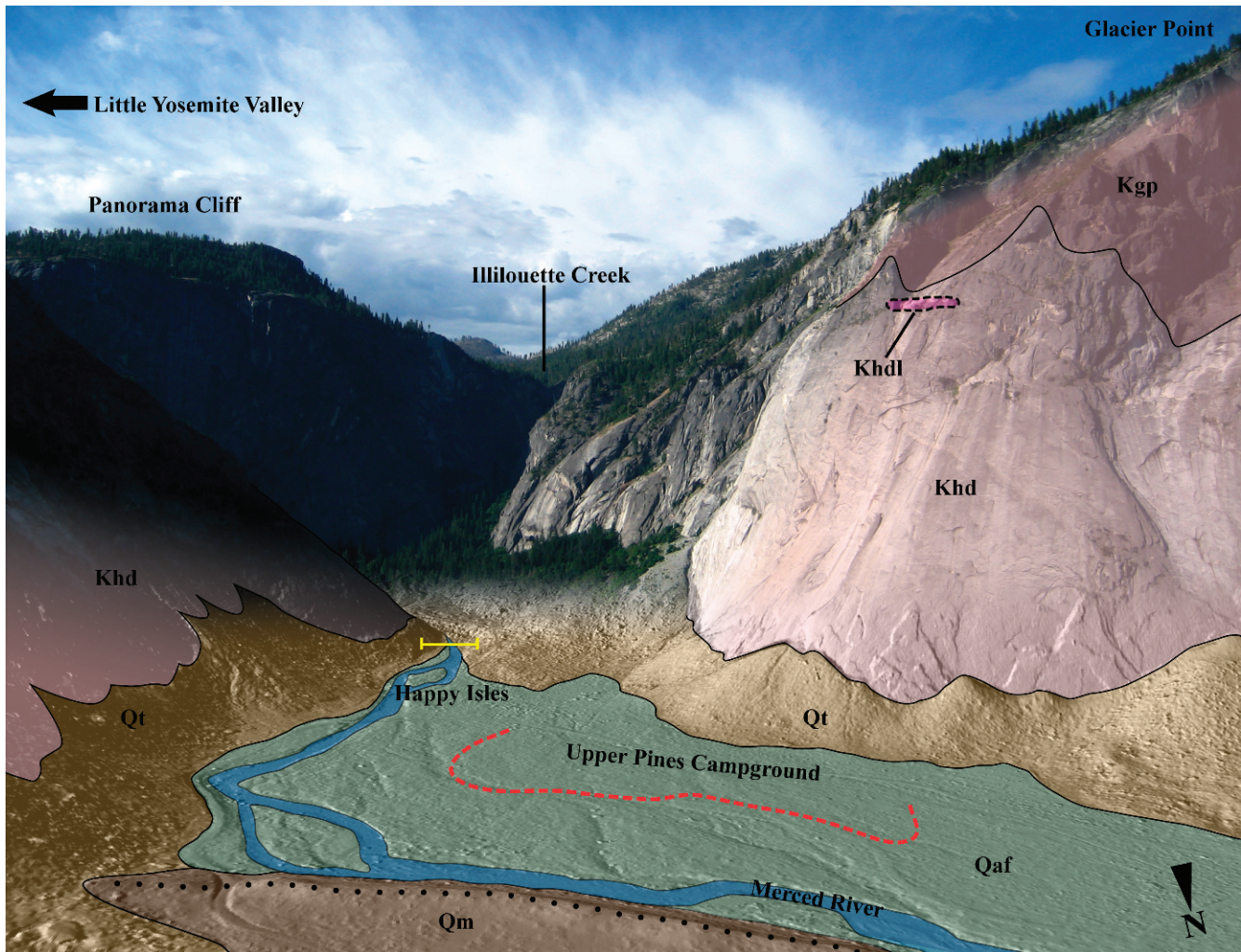


Figure 4. Photo of Glacier Point viewed from the northeast and overlain upon a hillshade produced from a 1 m LiDAR DEM, exposing the bare earth topography of the Upper Pines Campground alluvial fan. Granodiorite of Glacier Point–Half Dome Granodiorite boundary is from Peck (2002). Dashed red line marks the approximate boundary of mapped boulders within Upper Pines Campground; black dotted line represents the moraine crest; yellow line represents the cross section used for paleo-discharge and shear stress calculations. Qaf—alluvial fan, Qt—active talus, Qm—Last Glacial Maximum moraine, Khd—Half Dome Granodiorite, Khdl—leucocratic Half Dome Granodiorite, Kgp—granodiorite of Glacier Point.

within the fan surface (to confirm that boulders had not been moved during construction of the campground). We measured boulders by laying a tape measure on the ground with length and width perpendicular to each other. The highest point of a boulder was used to represent the minimum boulder height (minimum because the boulders are inset within the fan surface) and measured perpendicular to length and width. The GPS location of boulders has a ± 5 m accuracy. Boulders mapped using GPS were field checked for accuracy of location by measuring the distances of several prominent boulders to campground infrastructure in ArcGIS and comparing these measurements to walked paces in the field. We imported boulder location data into ArcGIS and reviewed their spatial relation to prominent

boulders resolved in a 1 m digital elevation model (DEM) derived from airborne light detection and ranging (LiDAR) (Stock et al., 2011).

Using the 1 m LiDAR DEM, we compiled previous mapping by Calkins et al. (1985), Alpha et al. (1987), Wiczorek et al. (1999), and Peck (2002) to create a detailed geologic map of the eastern extent of Yosemite Valley, focusing on the Upper Pines Campground area (Figure 4). We imported all 519 mapped boulders into ArcGIS and filtered out all boulders calculated to be $< 1 \text{ m}^3$ to evaluate spatial trends of boulders within the campground. We plotted the 270 filtered boulders ($> 1 \text{ m}^3$) by exposed volume, occupied surface area of the fan, and height (Figure 5).

As discussed in the results section, X-ray fluorescence (XRF) analysis revealed a geochemical anomaly

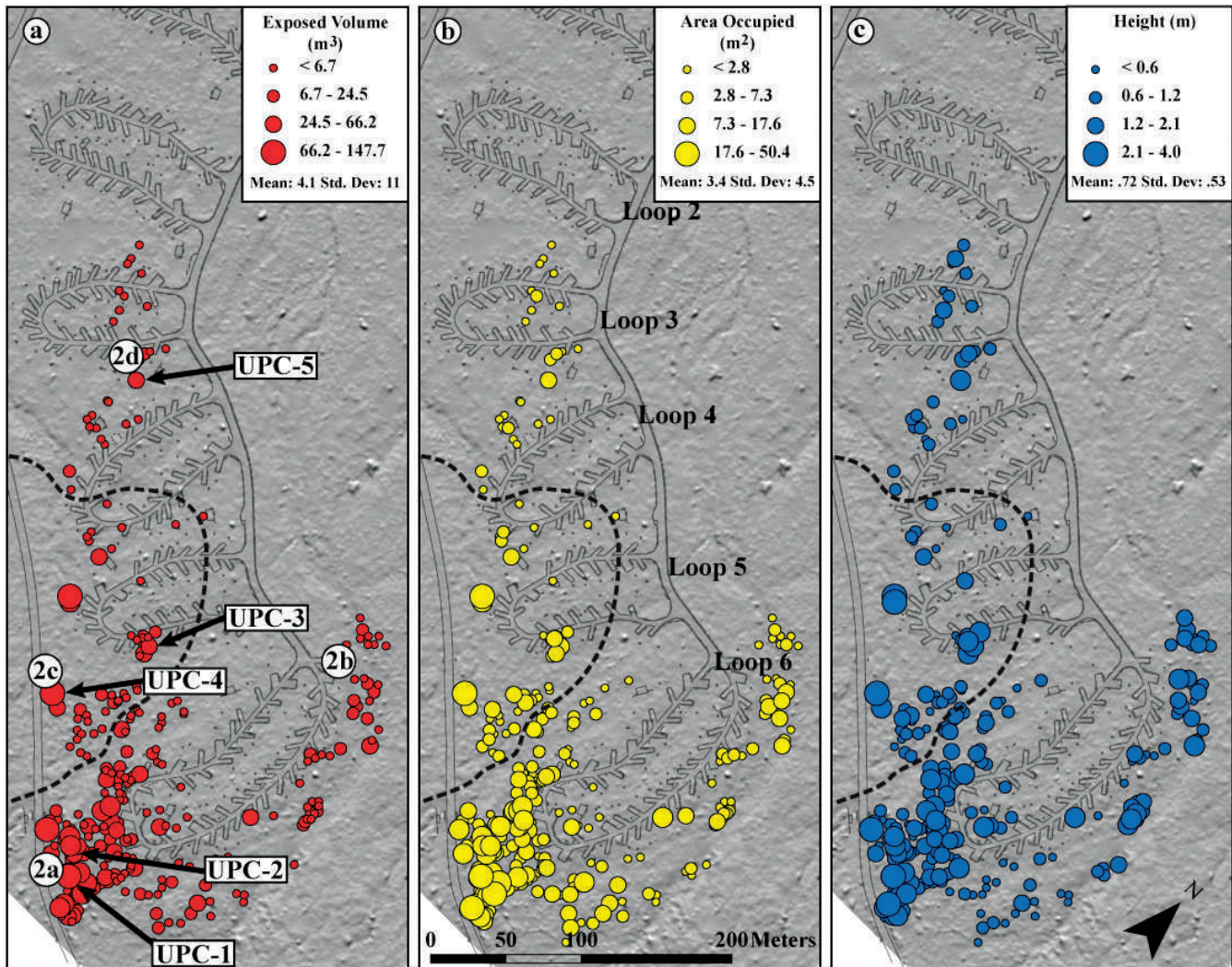


Figure 5. Mapped boulders $>1 \text{ m}^3$ in volume within Upper Pines Campground, Figure 2 photo locations, and sample sites for cosmogenic nuclide exposure dating. (a) Boulders plotted by exposed volume. (b) Boulders plotted by occupied surface area. (c) Boulders plotted by exposed height. Note the increasing orders of magnitude from northwest to southeast, particularly in panels a and b. Dashed line is extent of Wieczorek et al. (1999) debris flow.

in a boulder sampled in Upper Pines Campground that matched data from the leucocratic Half Dome Granodiorite obtained by Coleman et al. (2012). We began looking for a potential source on the Glacier Point cliff face using photographs and mapped an inferred zone of leucocratic Half Dome Granodiorite remotely using high-resolution gigapixel imagery of Yosemite Valley (xRez Studios, 2008; Stock et al., 2011). Comparing multiple photos taken at different sun angles with the xRez imagery, we concluded that the zone was more felsic than the surrounding cliff face due to its lithology rather than reflection of sunlight. While it is possible that this zone may appear more felsic than the cliff face due to its intersection with a prominent rock fall scar, dike swarming identified within the xRez imagery and directly below (east) a sharp upper contact (west)

suggests that this is a leucocratic zone of a felsic-mafic cycle (Coleman et al., 2012). Furthermore, this leucocratic zone is on strike with other mapped leucocratic zones (Coleman et al., 2012) and their projections into Tenaya Canyon.

Cosmogenic ^{10}Be Exposure Dating

To evaluate the timing of boulder deposition in Upper Pines Campground, we sampled five boulders for cosmogenic ^{10}Be exposure dating. This technique utilizes the accumulation of the cosmogenic isotope ^{10}Be in quartz exposed within $\sim 1 \text{ m}$ of Earth's surface by cosmic ray bombardment (Lal, 1991; Gosse and Phillips, 2001). Large rock fall deposits are generally well suited for ^{10}Be exposure dating because rock falls are essentially instantaneous events that excavate

rocks from deep (>1 m) within a cliff face (Ballantyne and Stone, 2004, 2013; Ivy-Ochs et al., 2009; and Stock and Uhrhammer, 2010). Vertical cliffs receive relatively low doses of cosmic rays due to the incidence angle of incoming cosmic rays, and most rock falls >1 m in thickness produce boulders on which faces were likely shielded within the cliff prior to failure, thereby reducing the possibility of ^{10}Be accumulation prior to failure. Due to the wide and flat floor of Yosemite Valley, the low gradient of the Merced River in the area, and the very low rates of boulder erosion, rock fall debris deposited on the valley floor since deglaciation is typically very well preserved.

Potentially complicating factors for cosmogenic nuclide exposure dating of boulders include nuclide loss due to surface erosion of a boulder, rotation of a boulder after deposition, rock spallation from forest fires, and topographic, vegetation, and snow shielding of cosmic rays (Gosse and Phillips, 2001; Ivy-Ochs et al., 2009). To address those issues, we collected samples from the top of large boulders generally positioned above the influence of fire-induced spallation. We accounted for topographic shielding (a significant concern due to the ~1-km-tall cliffs of Yosemite Valley) by making detailed measurements of the angle to the skyline from the exact sample location on a boulder. We assumed snow and vegetation shielding to be negligible and applied a boulder erosion rate of 0.00065 cm/yr (Small et al., 1997; Stock et al., 2005; and Stock and Uhrhammer, 2010).

Chemical preparation of ^{10}Be samples was performed at the Georgia Institute of Technology following standard methods (Kohl and Nishiizumi, 1992). Mass spectrometer analysis of ^{10}Be concentrations was performed by the Center for Accelerator Mass Spectrometry at Lawrence Livermore National Laboratories. We calculated cosmogenic nuclide exposure ages using the CRONUS age calculator (Balco et al., 2008).

X-Ray Fluorescence Spectrometry

Bedrock outcrops of granodiorite of Glacier Point at the summit of Glacier Point typically display the weak foliation, equigranular texture, and higher mafic mineral percentage of Peck's (2002) description. However, bedrock outcrops of Half Dome Granodiorite adjacent to Upper Pines Campground also locally have a weak foliation, variations that create an appearance similar to granodiorite of Glacier Point. Coleman et al. (2005) noted that the contact between the Half Dome Granodiorite and tonalite of Glen Aulin (equivalent to the granodiorite of Glacier

Point) is gradational in many places, and such gradation is likely in Yosemite Valley. In the context of what is observed within the boulders of Upper Pines Campground, mafic minerals range from 8 to 25 percent and contain both foliated and non-foliated grains, thus incorporating aspects of both granodiorite of Glacier Point and Half Dome Granodiorite. This often led to inconclusive field identification of boulders in Upper Pines Campground, with only Cathedral Peak Granodiorite readily identifiable.

To determine chemical affinity between granodiorite of Glacier Point and Half Dome Granodiorite, we collected 36 hand samples from boulders in Upper Pines Campground and from the adjacent bedrock cliffs and analyzed them using X-ray fluorescence (XRF) spectrometry. Of the 36 samples, eight *in situ* samples of granodiorite of Glacier Point were collected to create a geochemical database, identify variability within this unit, and provide a basis for comparison with boulder samples from the campground. Six of the samples were collected along the summit ridge of Glacier Point, and two samples were collected near the location where the contact between granodiorite of Glacier Point and Half Dome Granodiorite intersects the valley floor, west of Curry Village near Le Conte Gully. These samples encompass the lateral variation along the summit of the ridge of Glacier Point, and the vertical variation from the summit to the valley floor. Nine *in situ* samples of Half Dome Granodiorite bedrock adjacent to Upper Pines Campground were collected to identify local variability. XRF samples were analyzed at the University of North Carolina, Chapel Hill, on a Rigaku Supermini wavelength-dispersive XRF spectrometer using a lithium metaborate-tetraborate fusion.

RESULTS

Cosmogenic ^{10}Be Exposure Ages

Four out of the five boulders sampled for cosmogenic nuclide exposure dating (samples UPC-1, 2, 3, and 5) yield cosmogenic ^{10}Be exposure ages between 8.9 ± 0.8 and 10.9 ± 1.0 ka (Table 1). These four exposure ages overlap within external analytical uncertainty and yield a reduced χ^2 value of 0.83 and a probability of 0.48 (the probability that the analytical uncertainty accounts for all of the observed variance). These values suggest that the four exposure ages represent a single event with an unweighted mean exposure age of 9.6 ± 1 ka (Figure 6). The fifth boulder (sample UPC-4) has an exposure age of 5.7 ± 0.5 ka, considerably younger than—and statistically distinct from—the other four boulders (Figure 6).

Table 1. Cosmogenic beryllium-10 data and exposure ages for Upper Pines Campground boulders.

Sample	Lat/Long (°N/°W)	Elevation (m)	Thickness ^a (cm)	¹⁰ Be Production Rate (atoms/g/yr)		Shielding Factor ^d	Erosion Rate (cm/yr)	Mass Quartz (g)	Be Carrier (mg)	¹⁰ Be/ ⁹ Be ^{e,f} (× 10 ⁻¹³)	Concentration ^{f,g,h} (10 ⁴ atoms/g SiO ₂)	Exposure Age ^{i,j,k} (ka)
				Spallation ^b	Muons ^c							
UPC-1	37.7327/119.5608	1226	4	9.69	0.269	0.9180	0.00065	99,780	0.3897	3.95 ± 0.08	10.23 ± 0.23	10.90 ± 1.04
UPC-2	37.7330/119.5606	1225	3.5	9.85	0.269	0.9295	0.00065	99,500	0.3913	3.54 ± 0.11	9.21 ± 0.33	9.59 ± 0.95
UPC-3	37.7342/119.5617	1222	3	9.76	0.269	0.9197	0.00065	100,068	0.4090	3.25 ± 0.06	8.80 ± 0.19	9.23 ± 0.87
UPC-4	37.7336/119.5620	1223	4.5	9.44	0.268	0.8995	0.00065	100,495	0.4060	2.02 ± 0.04	5.37 ± 0.12	5.71 ± 0.53
UPC-5	37.7356/119.5636	1218	2	9.82	0.269	0.9200	0.00065	94,103	0.4080	2.98 ± 0.06	8.55 ± 0.19	8.90 ± 0.84

^aThe tops of all samples were exposed at the boulder surface.

^bConstant (time-invariant) local production rates based on Lal (1991) and Stone (2000). A sea-level, high-latitude value of 4.8 ¹⁰Be g⁻¹ quartz was used.

^cConstant (time-invariant) local production rate based on Heisinger et al. (2002a, 2002b).

^dGeometric shielding correction for topography and sample surface orientation calculated with the Cosmic-Ray Produced Nuclide Systematics (CRONUS) Earth online calculator (Balco et al., 2008) version 2.2 (<http://hess.ess.washington.edu/>).

^eIsotope ratios were normalized to ¹⁰Be standards prepared by Nishiizumi et al. (2007) with a value of 2.85 × 10¹² and using a ¹⁰Be half-life of 1.36 × 10⁶ years.

^fUncertainties are reported at the 1σ confidence level.

^gA mean blank value of 53,540 ± 10,845 ¹⁰Be atoms (¹⁰Be/⁹Be = 3.33 × 10⁻¹⁵ ± 8.74 × 10⁻¹⁶) was used to correct for background.

^hPropagated uncertainties include error in the blank, carrier mass (1 percent), and counting statistics.

ⁱPropagated error in the model ages include a 6 percent uncertainty in the production rate of ¹⁰Be and a 4 percent uncertainty in the ¹⁰Be decay constant.

^jA density of 2.7 g cm⁻³ was used based on the granitic composition of the samples.

^kBeryllium-10 model ages were calculated with the Cosmic-Ray Produced Nuclide Systematics (CRONUS) Earth online calculator (Balco et al., 2008) version 2.2 (<http://hess.ess.washington.edu/>).

X-Ray Fluorescence Analysis

Half Dome Granodiorite data were compiled with previous XRF analyses of Half Dome Granodiorite from Gray et al. (2008) and Coleman et al. (2012) and plotted in Harker diagrams (Figure 7). A comparison of the geochemistry of *in situ* bedrock samples to boulder samples in Upper Pines Campground allows for a more quantitative identification of boulders as either granodiorite of Glacier Point or Half Dome Granodiorite. More importantly, the comparisons show the spatial distribution of boulders with a known geochemical affinity.

In situ granodiorite of Glacier Point bedrock yields values of 57.5–58.2 weight percent SiO₂, contrasting with *in situ* Half Dome Granodiorite bedrock values from Gray et al. (2008) of 64.5–68.9 weight percent SiO₂ (Figure 7). A compositional gap of 61.9–64.9 weight percent SiO₂ for bedrock samples can be seen in Figure 7 between our *in situ* granodiorite of Glacier Point samples and the Half Dome Granodiorite data of Gray et al. (2008). We infer that due to the lack of additional *in situ* granodiorite of Glacier Point bedrock data, the range of 57.5–58.15 weight percent SiO₂ of collected bedrock samples likely does not represent the extent of variation within this unit. Instead, we estimate the range of granodiorite of Glacier Point to be 57.5–62.0 weight percent SiO₂ based on the separation seen in the Upper Pines boulder series (Figure 7) between 62.0 and 64.5 weight percent SiO₂.

Three of the four boulders sampled for cosmogenic nuclide exposure ages (samples UPC-2, 4, and 5) fall within 57.5–62.0 weight percent SiO₂ range of granodiorite of Glacier Point, indicating a geochemical affinity with bedrock above the granodiorite of Glacier Point–Half Dome Granodiorite contact (~500 vertical m above Upper Pines Campground). However, due to the significantly younger exposure age of boulder sample UPC-4 (5.7 ± 0.5 ka), we do not consider this sample to be representative of the age or lithology of the majority of boulders mapped within Upper Pines Campground. UPC-1 falls directly within the Gray et al. (2008) Half Dome Granodiorite data, a result that prompted a second independent analysis yielding the same results. UPC-3 falls within the leucocratic Half Dome Granodiorite data defined by Coleman et al. (2012), thus indicating that a leucocratic zone may be located on the Glacier Point cliff face.

The results of the XRF analysis indicate that granodiorite of Glacier Point and Half Dome Granodiorite boulders are scattered throughout the campground and not concentrated in a single location, as would be expected if a rock fall occurred

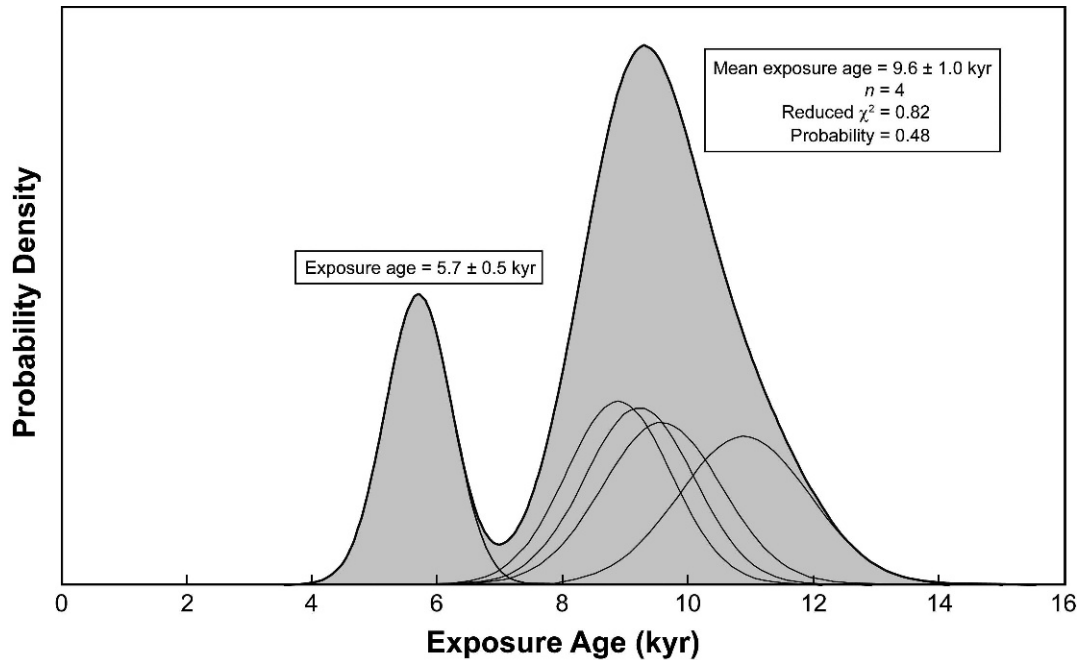


Figure 6. Probability density distributions of cosmogenic beryllium-10 exposure ages for boulders in Upper Pines Campground, with summary statistics. Individual boulder probability density distributions (black lines) are defined by the exposure age and the 1σ external uncertainty. Cumulative probability density distribution (gray curve) is calculated by summing the individual probability density distributions for all boulders. Results indicate two events, one at 5.7 ± 0.5 ka and another at 9.6 ± 1 ka. Retreat of the Last Glacial Maximum glacier from Yosemite Valley is inferred to have occurred circa 15–17 ka.

distinctly above or below the granodiorite of Glacier Point–Half Dome Granodiorite contact. Furthermore, all three mapped lithologies on Glacier Point are found within the campground and yield the same mean exposure age of 9.6 ± 1 ka. Three possible interpretations of the origin of boulders exposed in Upper Pines can be drawn from these results: (1) rock fall with a detachment zone crossing all three contacts or (2) fluvial or (3) debris flow mobilization of preexisting rock fall deposits encompassing all lithologies up valley from Upper Pines Campground.

DISCUSSION

The field and laboratory results described here provide data that can be used to test our four hypotheses for boulder deposition in Upper Pines Campground. Given that four boulder samples (UPC-1, 2, 3, and 5) have similar ^{10}Be exposure ages, we interpret these boulders as originating from the same event. XRF analysis of major elements identifies a compositional gap within the geochemical trend for granodiorite of Glacier Point and Half Dome Granodiorite bedrock samples, with boulders sampled (in Upper Pines Campground) falling on both sides of the gap. This suggests that granodiorite of Glacier Point boulders may have been moved by either slope processes (rock fall or debris flow) or fluvial processes.

Hypothesis 1: Glacial Deposit

Yosemite Valley was occupied by a glacier during the LGM, and, although the exact timing of deglaciation in the valley is not known, dating of moraines elsewhere in the Sierra Nevada suggest that deglaciation began at about 18–19 ka (Rood et al., 2011). In the adjacent Tuolumne River watershed, Clark (1976) estimated that glaciers retreated rapidly during deglaciation, and Dühnforth et al. (2010) showed that by 10–12 ka, glaciers had retreated to the highest elevations of the watershed. By inference, the glacier that occupied Yosemite Valley during the LGM had probably retreated from the valley by 15–17 ka (Huber, 1987; Wicczorek and Jäger, 1996). Since the mean cosmogenic nuclide exposure age of 9.6 ± 1 ka for the four older boulders in the Upper Pines Campground significantly post-dates the inferred timing of LGM deglaciation, it is highly unlikely that the boulders were deposited by glacier retreat.

Furthermore, the lithologies present in the Upper Pines Campground boulders are not those likely to have been deposited by the LGM glacier. XRF analysis identifies the presence of granodiorite of Glacier Point boulders in the deposit (Figure 7), a lithology that is not exposed up valley of Upper Pines Campground in Little Yosemite Valley, or below the

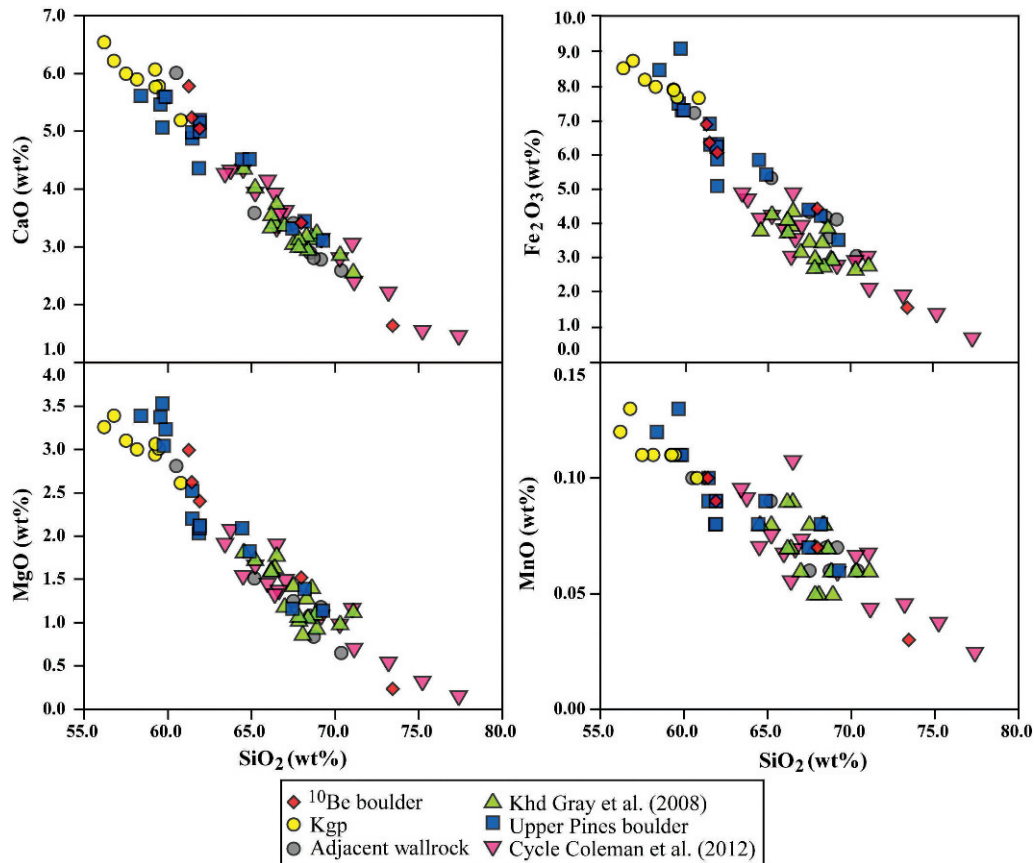


Figure 7. Harker variation diagrams of XRF analysis. Note the bedrock population compositional gap between *in situ* granodiorite of Glacier Point (yellow circles) and Half Dome Granodiorite (Gray et al., 2008; green triangles). Boulders sampled for ^{10}Be exposure ages (red diamonds) fall within both populations, as do samples collected in the Upper Pines Campground (blue squares). Note that while data of mafic-felsic cycles from Coleman et al. (2012) (pink triangles) extend the overall SiO_2 weight percent range of the Half Dome Granodiorite unit, it is considered a sub-unit and not used to delineate the bedrock population gap between granodiorite of Glacier Point and Half Dome Granodiorite.

inferred LGM trimline in Yosemite Valley mapped by Alpha et al. (1987). Reconstruction of the extent of the LGM glaciation in Yosemite National Park by Alpha et al. (1987) shows that the lower portion of Illilouette Creek was not glaciated, suggesting that glaciers were incapable of transporting granodiorite of Glacier Point boulders from up valley to Upper Pines Campground. Boulders of Cathedral Peak Granodiorite $>1 \text{ m}^3$ in volume are not found in Upper Pines Campground, in contrast to all other recognized glacial deposits in Yosemite Valley (Matthes, 1930; Huber, 1987). This diminishes the possibility that the boulders in Upper Pines Campground were exhumed from ground moraines.

Hypothesis 2: Flood Deposit

Given that the boulders in Upper Pines Campground are imbedded within an alluvial fan of the Merced River, we investigated the possibility that these boulders were deposited fluvially, most likely

during a glacial outburst flood or similar high-discharge flood event. We used the Manning's equation (Knighton, 1998) to estimate discharge and flow velocity for three different water depths along a cross section located at a confined portion of the valley where the gradient abruptly changes (Figure 4). We then calculated the bed stress generated by water depths of 5 m, 10 m, and 15 m, and the critical shear stress (Knighton, 1998) required to entrain boulders $\leq 1.4 \text{ m}$ and $\leq 3.5 \text{ m}$ in diameter. These diameters, which are those of sample boulders UPC-1 (Figure 2a) and UPC-5 (Figure 2d), respectively, were used to represent the minimum and maximum size of boulders entrained because of their known exposure age, lithology, and location on the alluvial fan. If a large discharge flood or glacial outburst event had occurred, both boulders must have been entrained to reach their current locations.

We calculated slope along the thalweg of the modern Merced River channel from Happy Isles Bridge to a point $\sim 600 \text{ m}$ upriver, which is the

Table 2. Discharge and bed stress calculations for the Merced River in the vicinity of Happy Isles.

Boulder Diameter (m)	Bottom Width (m)	Top Width (m)	Depth (m)	Cross-Sectional Area (m ²)	Manning's	Mean Velocity (m/s)	Discharge (m ³ /s)	Shear Stress (N/m ²)	Critical Shear Stress (N/m ²)
	w_1	w_2				v_1			
1.4	50	70	5	300	0.1	5.0	1,494	1,422	1,360
1.4	50	95	10	725	0.1	7.9	5,731	2,845	1,360
1.4	50	140	15	1,425	0.1	10.4	14,760	4,267	1,360
3.5	50	70	5	300	0.1	5.0	1,494	1,422	3,399
3.5	50	95	10	725	0.1	7.9	5,731	2,845	3,399
3.5	50	140	15	1,425	0.1	10.4	14,760	4,267	3,399

location of the cross section used to calculate discharge and bed shear stress (Figure 4). We chose this cross section because of its interaction with several large talus slopes capable of delivering granodiorite of Glacier Point and Half Dome Granodiorite boulders directly to the river channel. If a large glacial outburst flood or similarly large discharge flood occurred, it would need to entrain boulders composed of granodiorite of Glacier Point, Half Dome Granodiorite, and leucocratic Half Dome Granodiorite because all three lithologies are present within Upper Pines Campground. However, based on our method of mapping leucocratic Half Dome Granodiorite, it is inconclusive whether this zone would extend far enough up valley to allow for boulders to reach the channel above this cross section. For the sake of this argument, we will assume that this leucocratic zone could deliver boulders to the channel. Note that in our calculations, the dependent variable for critical basal shear stress is boulder diameter, whereas the dependent variables for bed load shear stress are flow depth and channel slope. In our calculations, we hold boulder diameter and channel slope constant and compare the critical basal shear stress generated by an increase in flow depth.

The results of shear stress calculations indicate that it is possible to generate and exceed the critical shear stress required (1360 N/m²) to entrain boulders with a diameter ≤1.4 m and ≤3.5 m within the confined cross section upstream of Upper Pines Campground (Table 2). However, water flowing downslope from the confined canyon of the cross section to the open alluvial fan would experience a substantial decrease in flow depth due to the much wider cross section at this location. This would lead to a substantial decrease in basal shear stress, thus immobilizing boulders. Therefore, it is unlikely that boulders could remain entrained beyond the confined cross section to reach their current locations on the alluvial fan at Upper Pines Campground. Although prehistoric flood events likely deposited boulders on the alluvial fan and modified the fan surface, they most likely did not

deposit boulders >1 m³. This would best explain why only small (<0.5 m³) boulders of Cathedral Peak Granodiorite are found on the fan surface.

The largest historical (A.D. 1851 to present) flood event recorded in Yosemite Valley occurred on 2 January 1997, with a peak discharge of ~283 m³/s and depth of approximately 4 m at Happy Isles. This flood corresponds to an approximately 100-year flood event. The 1997 flood did not inundate Upper Pines Campground and was several orders of magnitude lower in discharge than the discharge needed to mobilize the boulders in Upper Pines Campground (Table 2). Intact moraines in Little Yosemite Valley suggest that high-discharge flood events similar to that required to entrain boulders have not occurred upstream in Little Yosemite Valley since the LGM. A cutbank in the Merced River exposing the inner fan near Happy Isle Bridge reveals boulders no larger than ~1 m³, further suggesting that deposition of boulders >1.4 m in diameter from a large flood event is unlikely.

Hypothesis 3: Debris Flow Deposit

Wieczorek et al. (1999) mapped some of the boulders in Upper Pines Campground as a debris flow deposit originating from the east face of Glacier Point. While a debris flow originating from this area could deliver all three lithologies to the campground area, making it a plausible explanation for the origin of boulders, mapping by Wieczorek et al. (1999) only accounts for boulders located in one portion of the study area, and excludes the largest density of boulders that we mapped (Figure 5). Sample boulder UPC-3 is included within Wieczorek et al.'s (1999) mapped debris flow deposit and matches the exposure ages of sample boulders UPC-1, 2, and 5, indicating that either the full extent of the deposit was unrecognized by Wieczorek et al. (1999), or that boulders were deposited by a different process.

The surface morphology of other debris flow fans in Yosemite Valley, such as those at Eagle Creek (Figure 3b), Sentinel Creek, Indian Creek, and

Le Conte Gully, displays a readily distinguishable cone-shaped morphology, a rough channelized surface with V-shaped or rectangular channel cross sections, and lateral ridges of coarse rock debris (Bertolo and Wieczorek, 2005). In areas of these debris flow fans that contain boulders of similar size to those in Upper Pines Campground, surface slopes on the fans are on the order of 7 degrees to 24 degrees. This contrasts markedly with the much lower surface slope of 0.8 degrees along the apex of the alluvial fan surface at Upper Pines Campground, and the fan surface slope of 0.4 degrees derived from the apex of the debris flow mapped by Wieczorek et al. (1999). This further suggests that debris flows were not the origin of the boulders in Upper Pines Campground.

Hypothesis 4: Rock Fall Deposit

The available evidence suggests rock fall to be the most likely origin for the boulders in Upper Pines Campground. As a rock fall deposit could be preserved on the valley floor any time after deglaciation circa 15–17 ka, a mean exposure age of 9.6 ± 1 ka for the older boulders is consistent with rock fall deposition.

The spatial distribution of boulders in Upper Pines Campground, as well as their lithologic compositions, suggests that the source of this rock fall was on the eastern flank of Glacier Point. Both the granodiorite of Glacier Point and Half Dome Granodiorite are present on the eastern flank of Glacier Point, and a zone of leucocratic Half Dome Granodiorite is inferred to exist just below the contact between the two (Figures 4 and 8). Because all of these lithologies are present in the Upper Pines boulders, we interpret that the rock fall source area must have crossed the contact between all three units. We identify a possible source area along this contact, positioned directly above the deposit, that coincides with an obvious gap in the topography formed along pervasive east-dipping (dip slope) joints (Figure 8). The geological contacts in this area may have contributed to slope failure, as noted elsewhere (Weidinger and Korup, 2009). The eastern flank of Glacier Point has experienced several historical (A.D. 1857 to present) rock falls (Stock et al., 2013), including an $\sim 30,000$ m³ rock fall on 10 July 1996 that devastated the Happy Isles area with an air blast and dense sandy cloud (Wieczorek et al., 2000).

The farthest extent of boulders in Upper Pines Campground is ~ 300 m beyond the base of the active talus slope beneath Glacier Point and ~ 500 m from the base of the cliff, demonstrating the long run-out distance of this rock fall. Although we have not

modeled the dynamics of this rock fall, it is likely that the long run-out distance results from both the initial large volume of the deposit (e.g., Okura et al., 2000) and the moderately dipping (~ 60 degrees) topography of the Glacier Point apron beneath the inferred rock fall source area (Figure 8), which would tend to more effectively translate initial vertical momentum into horizontal momentum.

Typical deposits resulting from extremely large rock falls in Yosemite Valley are characterized by a dense cover of angular boulders with a pronounced distal edge and hummocky topography within the body of the deposit (Stock and Uhrhammer, 2010). Although the surface morphology of the boulder deposit in Upper Pines Campground does not strongly resemble any other boulder deposit of known origin in Yosemite Valley, it most closely resembles deposits mapped by Wieczorek et al. (1999) as extremely large rock falls (rock avalanches), in particular those located near Sugarpine Bridge and Old Yosemite Village. We suggest that the boulder deposit in Upper Pines Campground may have once exhibited a similar morphology, but that much of the deposit has subsequently been buried by alluvial fan aggradation, reducing its surface expression. Several lines of evidence support this interpretation.

First, post-glacial sediment aggradation of the floor of Yosemite Valley has been quantified at a location 1.7 km northwest of Upper Pines Campground (Figure 1). Gerald Wieczorek of the U.S. Geological Survey and colleagues collected two charcoal fragments from the cutbank of a terrace adjacent to the Merced River downstream of Stoneman Bridge (Figure 1). The samples were located ~ 2.5 m below the terrace surface within an ~ 50 -cm-thick sequence of alternating layers of fine to coarse silt, interpreted as lake deposits, and containing trace amounts of fluviially transported tephra (G. F. Wieczorek and A. M. Sarna-Wojcicki, pers. commun., 1999) (Figure 9). The two charcoal samples were analyzed for radiocarbon and yielded calibrated (Stuiver et al., 1986) ages of 10.5–11.7 kyr B.P., with a median age 11.1 kyr B.P. These data suggest that ≥ 2.5 m of alluvial aggradation occurred at this location after deposition of the charcoal fragments circa 11.1 ka and prior to incision of the valley floor. Because the mean exposure age of boulders within Upper Pines Campground is only slightly younger than the median radiocarbon age of the charcoal, we infer that the boulders were most likely deposited during the aggradation phase preceding incision of the valley floor. If correct, then the rock fall deposit at Upper Pines Campground was likely subjected to at least 2.5 m of sediment aggradation after it was deposited. We posit that the amount of aggradation was likely

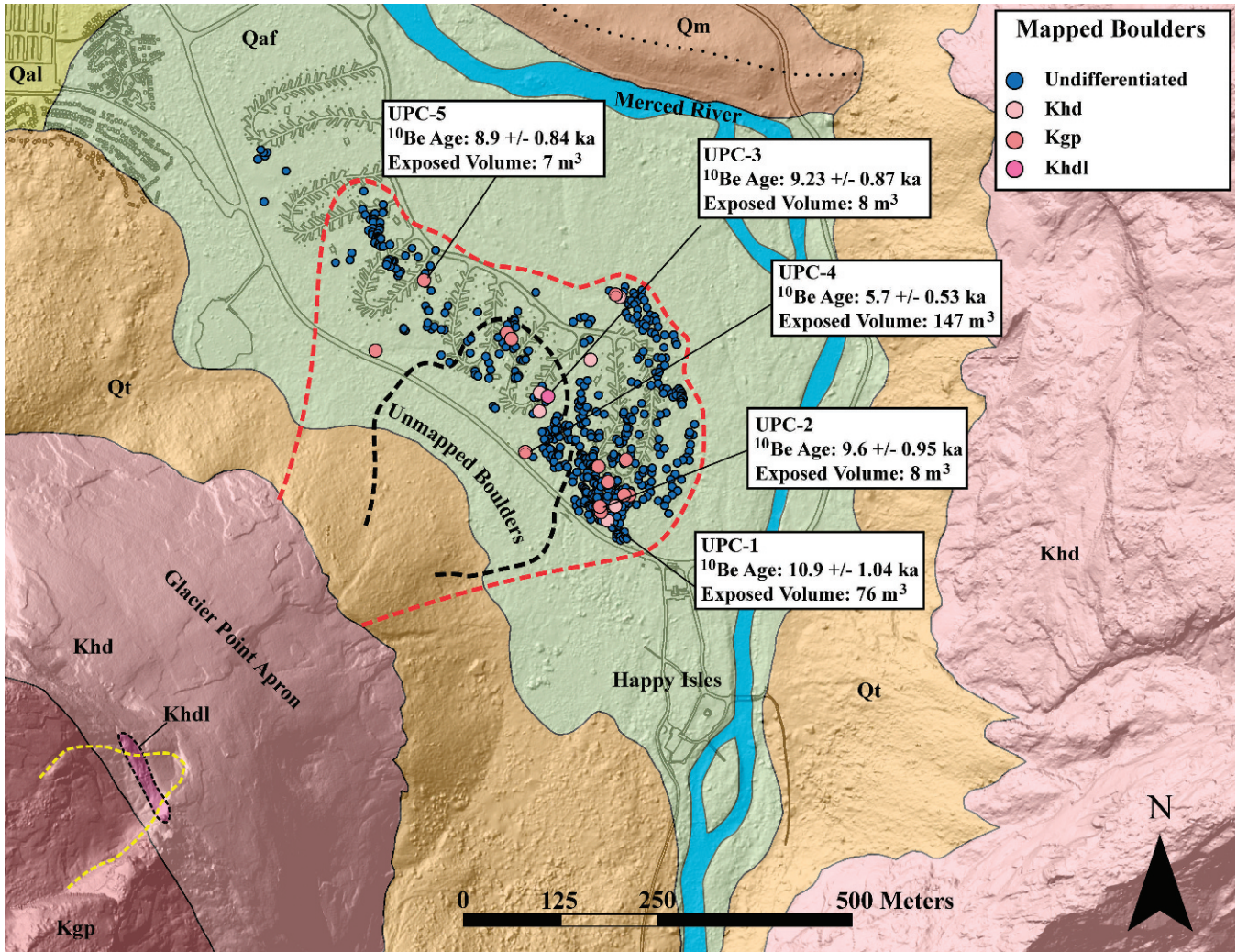


Figure 8. Geologic map of Upper Pines Campground and vicinity, showing boulder locations, mapped lithologies, and cosmogenic nuclide exposure ages. Dashed yellow line delineates a possible rock-fall source area within a topographic gap that crosses the three lithologic units represented in mapped boulders; dashed black line is the extent of the debris flow mapped by Wieczorek et al. (1999); dashed red line is the inferred extent of the 9.6 ± 1 ka rock fall event. Qal—alluvium, Qaf—alluvial fan, Qt—active talus, Qm—LGM moraine, Khd—Half Dome Granodiorite, Khdl—leucocratic Half Dome Granodiorite, Kgp—granodiorite of Glacier Point.

greater than 2.5 m in the Upper Pines Campground area, given that this location is on the alluvial fan, where coarse (gravel and cobble-sized) sediment deposition has been more prevalent than near Stone-man Bridge.

Boulder height, occupied area, and exposed volume decrease from southeast to northwest in the down-stream direction of the alluvial fan (Figure 5). The inset appearance and relatively small exposed volume of boulders in the northern portion of the camp-ground may best be explained by partial burial of boulders during fan development subsequent to boulder deposition. Figure 5 displays an increase in magnitude of boulder attributes arcing around campground loop 6. This is likely due to a small seasonal channel that has incised into the fan and

exposed these boulders, indicating that the fan surface directly occupied by Upper Pines Campground is composed of large and highly inset boulders, which give a visual appearance of small boulders on the surface (Figure 2b). As previously stated, a cutbank near Happy Isle Bridge exposes boulders of the inner fan <1 m³, indicating that buried boulders of the Upper Pines Campground rock fall deposit end between campground loop 6 and the modern-day Merced River.

The cumulative exposed volume of boulders mapped within Upper Pines Campground is approximately 2,100 m³. However, as described earlier herein, this is likely a minimum volume due to post-deposition aggradation of the alluvial fan. As an example of the effect sediment aggradation may have

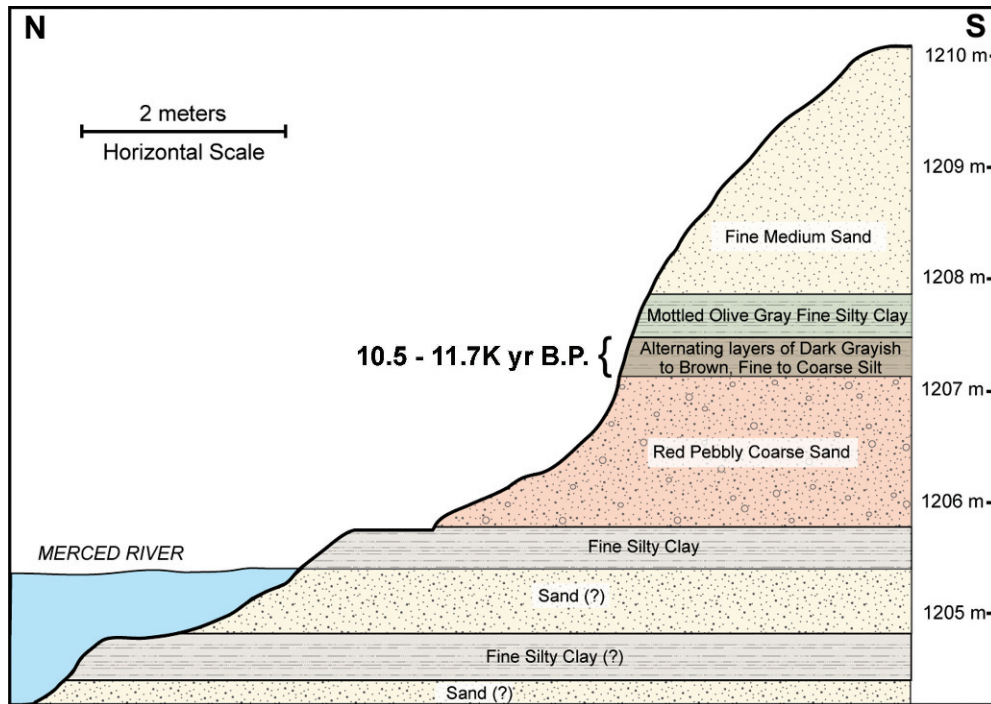


Figure 9. Stratigraphic column of riverbank sediments adjacent to the Merced River downstream of Stoneman Bridge. Two charcoal fragments between 1207.0 and 1207.5 m elevation yield calibrated radiocarbon ages between 10.5 and 11.7 kyr B.P. Radiocarbon ages and stratigraphic column are courtesy of G. F. Wiczeorek (pers. commun., 1999).

on exposed boulder volume, Stock and Uhrhammer (2010) calculated a volume for the distal portion of the 3.6 ka El Capitan Meadow rock avalanche, located approximately 6.5 km east of Upper Pines Campground, of about 1.03 million m^3 ; these values were calculated based on the present valley floor elevation of 1204 m. If the present valley floor elevation were to aggrade by 5 m (derived from the elevation of terraces above the modern-day channel of the Merced River in eastern Yosemite Valley) to 1209 m above mean sea level (amsl) elevation, the exposed volume of this deposit would decrease by roughly half. We suggest that a similar scenario has already occurred in Upper Pines Campground, with a substantial (but as yet unresolved) volume of the deposit buried beneath alluvium over the past 9.6 ka.

Assessment of Rock-Fall Hazard

If the boulders in Upper Pines Campground are indeed of rock fall origin, then the campground is plausibly subject to similar events in the future. However, the boulder exposure ages indicate that an event of this extent has happened only once at this location since the retreat of the LGM glacier, yielding a frequency of 1 in about 15–17 ka. Because the inferred frequency of this size event is low, the actual hazard posed by rock falls to most of Upper Pines

Campground is also relatively low. However, the younger age of sample UPC-4 (5.7 ± 0.5 ka) on the western edge of the campground suggests that this boulder was deposited by a more recent rock fall from Glacier Point. Evidence for at least two rock falls at this location increases the frequency of occurrence there and thus elevates the hazard; this is consistent with the well-documented notion that rock-fall hazard increases with proximity to the edge of the active talus slope (e.g., Evans and Hungr, 1993).

The probability of future extremely large rock falls in Yosemite Valley may be most directly tied to local seismic recurrence intervals. Earthquakes are known triggers of rock falls, especially extremely large rock falls and rock avalanches (e.g., Keefer, 1984). Earthquakes have triggered at least 25 rock falls in Yosemite since A.D. 1857, although these represent only a small proportion (~3%) of all documented rock falls, highlighting the importance of other triggering mechanisms (Stock et al., 2013). Stock and Uhrhammer (2010) tentatively correlated the El Capitan Meadow rock avalanche with a large ($M > 7.0$) rupture of the Owens Valley Fault circa 3.6 ka (Lee et al., 2001). Based on dated offset stratigraphy, Bacon and Pezzopane (2007) constrained the timing of an earlier rupture of the Owens Valley Fault to between 8.8 ± 0.2 and 10.2 ± 0.2 kyr B.P., with a median age of 9.5 ± 0.9 kyr B.P. This age

corresponds to the mean exposure age of boulders in Upper Pines Campground at 9.6 ± 1 ka. As with the El Capitan Meadow rock avalanche event, we cannot confidently correlate the earliest Holocene rupture event of the Owens Valley Fault with the rock fall from Glacier Point, nor can we exclude other possible triggering mechanisms, such as water pressure, freeze-thaw, etc., which have been important triggers historically (Stock et al., 2013). However, given the inferred large size of the deposit, the temporal correspondence with a known rupture of the Owens Valley Fault, and the fact that the 1872 Owens Valley earthquake triggered at least six rock falls in Yosemite Valley (Stock et al., 2013), we tentatively suggest that the 9.6 ± 1 ka rock fall from Glacier Point may have been triggered by an earthquake along the Owens Valley Fault. If correct, then the hazard posed by extremely large rock falls in Yosemite may be largely dependent on the frequency and magnitude of earthquakes along the eastern Sierra Nevada frontal fault system.

CONCLUSIONS

We evaluated four hypotheses for the deposition of enigmatic boulders in Upper Pines Campground: (1) glacial deposition during retreat of the LGM glacier in Yosemite Valley, (2) fluvial deposition during a glacial outburst or similar large-discharge flood event, (3) deposition by a debris flow, or (4) deposition by an extremely large rock fall.

The balance of evidence suggests that a rock fall is the most likely origin for these boulders. XRF analyses of boulders and bedrock strongly suggest that the source of boulders was from near the contact of granodiorite of Glacier Point, Half Dome Granodiorite, and the inferred location of leucocratic Half Dome Granodiorite. All lithologies are exposed above and west of Upper Pines Campground in a rock fall scar. Four out of five boulder exposure ages are similar and yield a mean age of 9.6 ± 1 ka. This age is considerably younger than the inferred timing of LGM deglaciation from Yosemite Valley. River discharge and bed shear stress calculations indicate that fluvial deposition of boulders is highly unlikely because of the unrealistically large discharge required for sustained (~1 km) boulder entrainment. Although we cannot rule out deposition by debris flows, the boulders in Upper Pines Campground rest on considerably lower slopes than boulders of similar size on known debris flow fans elsewhere in Yosemite Valley.

Based on the distribution, age, and lithologic composition of the boulders, we posit that the most likely explanation is that these boulders were simultaneously deposited by a rock fall from Glacier Point

9.6 ± 1 ka, and the extent of mapped boulders best resembles a rock avalanche. A boulder on the western edge of the deposit with an exposure age of 5.7 ± 0.5 ka appears to be unrelated to the majority of boulders in the campground and likely results from a more recent rock fall.

Based on XRF analysis of boulders and the adjacent bedrock, we interpret the rock fall as originating from the eastern flank of Glacier Point from a source area that crossed all three lithologic units (Figures 4 and 7). The spatial distribution of exposed boulder volume, occupied surface area, and boulder height suggest that this deposit was subsequently partially buried by alluvial fan aggradation, and that only a fraction of the original deposit is presently exposed on the surface of the fan (Figure 5).

ACKNOWLEDGMENTS

We thank Bud Burke, Andre Lehre, Harvey Kelsey, and Sue Cashman for providing helpful suggestions, assistance, and guidance. Jim Snyder offered valuable insights into the nature of rock falls in the Happy Isles area. Codie LaPoint and Casey Cordes assisted with field work. Tom Chapman prepared the XRF samples at the University of North Carolina, Chapel Hill. Tina Marsteller prepared the ¹⁰Be samples at the Georgia Institute of Technology, and Dylan Rood performed the ¹⁰Be analyses at Lawrence Livermore National Laboratories. Gerald Wiczorek and Meghan Morrissey, of U.S. Geological Survey collected the radiocarbon samples near Stoneman Bridge, along with Jack Knierieman and Jim Snyder of the National Park Service. Jack McGeehin of the U.S. Geological Survey radiocarbon laboratory performed the radiocarbon dating at the University of Arizona Accelerator Mass Spectrometry Laboratory. Additional interpretation of these samples and the adjacent stratigraphy near Stoneman Bridge was provided by Andre Sarna-Wojcicki and N. King Huber of the U.S. Geological Survey. We appreciate constructive reviews by John Duffy, Martin Woodward, and an anonymous reviewer. This research was supported by the National Park Service and the Yosemite Conservancy.

REFERENCES

- ALPHA, T. R.; WAHRHAFTIG, C.; AND HUBER, N. K., 1987, *Oblique Map Showing Maximum Extent of 20,000-Year-Old (Tioga) Glaciers, Yosemite National Park, Central Sierra Nevada, California*: U.S. Geological Survey Miscellaneous Investigations Series Map I-1885.
- BACON, S. N. AND PEZZOPANE, S. K., 2007, A 25,000-year record of earthquakes on the Owens Valley Fault near Lone Pine, California: Implications for recurrence intervals, slip rates,

- and segmentation models: *Geological Society of America Bulletin*, Vol. 119, pp. 823–847.
- BALCO, G.; STONE, J. O.; LIFTON, N. A.; AND DUNAI, T. J., 2008, A complete and easily accessible means of calculating surface exposure ages or erosion rates from ^{10}Be and ^{26}Al measurements: *Quaternary Geochronology*, Vol. 3, pp. 174–195.
- BALLANTYNE, C. K. AND STONE, J. O., 2004, The Beinn Alligin rock avalanche NW Scotland: Cosmogenic ^{10}Be dating, interpretation and significances: *The Holocene*, Vol. 14, pp. 448–453.
- BALLANTYNE, C. K. AND STONE, J. O., 2013, Timing and periodicity of paraglacial rock-slope failures in the Scottish Highlands: *Geomorphology*, Vol. 186, pp. 150–161.
- BATEMAN, P. C., 1992, *Plutonism in the Central Part of the Sierra Nevada Batholith, California*: U.S. Geological Survey Professional Paper 1483, 186 p.
- BATEMAN, P. C.; KISTLER, R. W.; PECK, D. L.; AND BUSACCA, A., 1983, *Geologic Map of the Tuolumne Meadows Quadrangle, Yosemite National Park, California*: U.S. Geological Survey Geologic Quadrangle Map GQ-1570, scale 1:62,500.
- BERTOLO, P. AND WIECZOREK, G. F., 2005, Calibration of numerical models for small debris flows in Yosemite Valley, California, USA: *Natural Hazards and Earth System Sciences*, Vol. 5, pp. 993–1001.
- BIRKELAND, P. W. AND BURKE, R. M., 1988, Soil catena chronosequences on eastern Sierra Nevada moraines, California, U.S.A.: *Arctic and Alpine Research*, Vol. 20, pp. 473–484.
- BURSIK, M. I. AND GILLESPIE, A. R., 1993, Late Pleistocene glaciation of Mono Basin, California: *Quaternary Research*, Vol. 39, pp. 24–35.
- CALKINS, F. C.; HUBER, N. K.; AND ROLLER, J. A., 1985, *Bedrock Geologic Map of Yosemite Valley, Yosemite National Park, California*: U.S. Geological Survey Miscellaneous Investigation Series Map I-1639, scale 1:24,000.
- CLARK, M., 1976, Evidence for rapid destruction of latest Pleistocene glaciers of the Sierra Nevada, California: *Geological Society of America Abstract with Programs*, Vol. 8, No. 3, pp. 361–362.
- COLEMAN, D. S.; GRAY, W.; AND GLAZNER, A. F., 2004, Rethinking the emplacement and evolution of zoned plutons: Geochronologic evidence for incremental assembly of the Tuolumne Intrusive Suite, California: *Geology*, Vol. 32, No. 5, pp. 433–436.
- COLEMAN, D. S.; BARTLEY, J. M.; GLAZNER, A. F.; AND LAW, R. D., 2005, Incremental assembly and emplacement of Mesozoic plutons in the Sierra Nevada and White and Inyo Ranges, California. In *Geological Society of America Field Forum Field Trip Guide: Rethinking the Assembly and Evolution of Plutons: Field Tests and Perspectives (7–14 October 2005)*: Geological Society of America, Boulder, CO, p. 59.
- COLEMAN, D. S.; BARTLEY, J. M.; GLAZNER, A. F.; AND PARDUE, M. J., 2012, Is chemical zonation in plutonic rocks driven by changes in source magma composition, or shallow crustal differentiation?: *Geosphere*, Vol. 8, pp. 1568–1587.
- DÜHNFORTH, M.; ANDERSON, R. S.; WARD, D.; AND STOCK, G. M., 2010, Bedrock fracture control of glacial erosion processes and rates: *Geology*, Vol. 38, pp. 423–426.
- EVANS, S. G. AND HUNGR, O., 1993, The assessment of rockfall hazard at the base of talus slopes: *Canadian Geotechnical Journal*, Vol. 30, pp. 620–636.
- GOSSE, J. C. AND PHILLIPS, F. M., 2001, Terrestrial *in situ* cosmogenic nuclides: Theory and application: *Quaternary Science Reviews*, Vol. 20, pp. 1475–1560.
- GRAY, W.; GLAZNER, A. F.; COLEMAN, D. S.; AND BARTLEY, J. M., 2008, Long-term geochemical variability of the Late Cretaceous Tuolumne Intrusive Suite, central Sierra Nevada, California. In Annen, C. and Zellmer, G. F. (Editors), *Dynamics of Crustal Magma Transfer, Storage, and Differentiation*: Special Publication 304, Geological Society of London, pp. 183–201.
- HEISINGER, B.; LAL, D.; JULL, A. J. T.; KUBIK, P.; IVY-OCHS, S.; NEUMAIER, S.; KNIEW, K.; LAZAREV, V.; AND NOLTE, E., 2002a, Production of selected cosmogenic radionuclides by muons: 1. Fast muons: *Earth and Planetary Science Letters*, Vol. 200, pp. 345–355.
- HEISINGER, B.; LAL, D.; JULL, A. J. T.; KUBIK, P.; IVY-OCHS, S.; KNIE, K.; AND NOLTE, E., 2002b, Production of selected cosmogenic radionuclides by muons: 2. Capture of negative muons: *Earth and Planetary Science Letters*, Vol. 200, pp. 357–369.
- HUBER, N. K., 1987, *The Geologic Story of Yosemite National Park*: U.S. Geological Survey Bulletin 1595, 64 p.
- HUBER, N. K. AND SNYDER, J. B., 2007, A history of the El Capitan moraine. In Huber, N. K. (Editor), *Geological Ramblings in Yosemite*: Heyday Books, Berkeley, CA, pp. 103–110.
- HUBER, N. K.; BATEMAN, P. C.; AND WAHRHAFTIG, C., 1989, *Geologic Map of Yosemite National Park and Vicinity, California*: U.S. Geological Survey Miscellaneous Investigations Series Map I-1874, scale 1:125,000.
- IVY-OCHS, S.; POSCHINGET, A. V.; SYNAL, H.-A.; AND MAISCH, M., 2009, Surface exposure dating of the Flims landslide, Graubünden, Switzerland: *Geomorphology*, Vol. 103, pp. 104–112.
- KEEFER, D. K., 1984, Landslides caused by earthquakes: *Geological Society of America Bulletin*, Vol. 95, pp. 406–421.
- KISTLER, R. C., 1973, *Geologic Map of the Hetch Hetchy Reservoir Quadrangle, Yosemite National Park, California*: U.S. Geological Survey Map GQ-1112, scale 1:62,500.
- KNIGHTON, D., 1998, *Fluvial Forms and Processes*: Oxford University Press, New York, pp. 96–105.
- KOHL, C. P. AND NISHIZUMI, K., 1992, Chemical isolation of quartz for measurement of *in-situ* produced cosmogenic nuclides: *Geochimica et Cosmochimica Acta*, Vol. 56, pp. 3583–3587.
- LAL, D., 1991, Cosmic ray labeling of erosion surfaces: *In situ* nuclide production rates and erosion models: *Earth and Planetary Science Letters*, Vol. 104, pp. 424–439.
- LEE, J.; SPENCER, J.; AND OWEN, L., 2001, Holocene slip rates along the Owens Valley Fault, California: Implications for the recent evolution of the Eastern California Shear Zone: *Geology*, Vol. 29, pp. 819–822.
- MATTHES, F. E., 1930, *Geologic History of the Yosemite Valley*: U.S. Geological Survey Professional Paper 160.
- NISHIZUMI, K.; IMAMURA, M.; CAFFEE, M. W.; SOUTHON, J. R.; FINKEL, R. C.; AND MCANINCH, J., 2007, Absolute calibration of ^{10}Be AMS standards: *Nuclear Instruments and Methods in Physics, Ser. B*, Vol. 258, pp. 403–413.
- OKURA, Y.; KITAHARA, H.; SAMMORI, T.; AND KAWANAMI, A., 2000, The effects of rockfall volume on runout distance: *Engineering Geology*, Vol. 58, pp. 109–124.
- PECK, D. L., 1980, *Geologic Map of the Merced Peak Quadrangle, Central Sierra Nevada, California*: U.S. Geological Survey Series Map GQ-1531, scale 1:62,500.
- PECK, D. L., 2002, *Geologic Map of the Yosemite Quadrangle, Central Sierra Nevada, California*: U.S. Geological Survey Geologic Investigations Series Map I-2751, scale 1:62,500.
- PHILLIPS, F. M.; ZREDA, M. G.; PLUMMER, M. A.; ELMORE, D.; AND CLARK, D. H., 2009, Glacial geology and chronology of Bishop Creek and vicinity, eastern Sierra Nevada, California: *Geological Society of America Bulletin*, Vol. 121, No. 7–8, pp. 1013–1033.
- ROOD, D. H.; BURBANK, D. W.; AND FINKEL, R. C., 2011, Chronology of glaciations in the Sierra Nevada, California,

9.6 ± 1 ka Rock Fall, Glacier Point, Yosemite Valley, California

- from ^{10}Be surface exposure dating: *Quaternary Science Reviews*, Vol. 30, pp. 646–661.
- SMALL, E. E.; ANDERSON, R. S.; REPKA, J. L.; AND FINKEL, R., 1997, Erosion rates of alpine bedrock summit surfaces deduced from *in situ* ^{10}Be and ^{26}Al : *Earth and Planetary Science Letters*, Vol. 150, pp. 413–425.
- STOCK, G. M.; ANDERSON, R. S.; AND FINKEL, R. C., 2005, Rates of erosion and topographic evolution of the Sierra Nevada, California, inferred from cosmogenic ^{26}Al and ^{10}Be concentrations: *Earth Surface Processes and Landforms*, Vol. 30, pp. 985–1006.
- STOCK, G. M.; BAWDEN, G. W.; GREEN, J. K.; HANSON, E.; DOWNING, B.; COLLINS, B. D.; BOND, S.; AND LESLAR, M., 2011, High-resolution three-dimensional imaging and analysis of rock falls in Yosemite Valley, California: *Geosphere*, Vol. 7, pp. 573–581.
- STOCK, G. M.; COLLINS, B. D.; SANTANIELLO, D. J.; ZIMMER, V. L.; WIECZOREK, G. F.; AND SNYDER, J. B., 2013, *Historical Rock Falls in Yosemite National Park, California (A.D. 1857–2011)*: U.S. Geological Survey Data Series Report 746 (in press).
- STOCK, G. M. AND UHRHAMMER, R. A., 2010, Catastrophic rock avalanche 3600 years BP from El Capitan, Yosemite Valley, California: *Earth Surface Processes and Landforms*, Vol. 35, pp. 941–951.
- STONE, J. O., 2000, Air pressure and cosmogenic isotope production: *Journal of Geophysical Research*, Vol. 105, pp. 23753–23759.
- STUIVER, A.; REIMER, P. J.; AND REIMER, R., 1986, *CALIB Radiocarbon Calibration*: Electronic document, available at <http://calib.qub.ac.uk/calib/>
- WAHRHAFTIG, C., 1962, *Geomorphology of the Yosemite Valley Region, California*. In *Geologic Guide to the Merced Canyon and Yosemite Valley, California*: California Division of Mines and Geology Bulletin 182, pp. 33–46.
- WEIDINGER, J. T. AND KORUP, O., 2009, Frictionite as evidence for a large Late Quaternary rockslide near Kachenjunga, Sikkim Himalayas, India—Implications for extreme events in mountain relief destruction: *Geomorphology*, Vol. 103, pp. 57–65.
- WIECZOREK, G. F. AND JÄGER, S., 1996, Triggering mechanisms and depositional rates of postglacial slope-movement processes in the Yosemite Valley, California: *Geomorphology*, Vol. 15, pp. 17–31.
- WIECZOREK, G. F.; MORRISSEY, M. M.; IOVINE, G.; AND GODT, J. W., 1999, *Rock-Fall Potential in the Yosemite Valley, California*: U.S. Geological Survey Open-File Report 99-578.
- WIECZOREK, G. F.; SNYDER, J. B.; WAITT, R. B.; MORRISSEY, M. M.; UHRHAMMER, R. A.; HARP, E. L.; NORRIS, R. D.; BURSIK, M. I.; AND FINWOOD, L. G., 2000, Unusual July 10, 1996, rock fall at Happy Isles, Yosemite National Park, California: *Geological Society of America Bulletin*, Vol. 112, pp. 75–85.
- XREZ STUDIOS, 2008, Yosemite Extreme Panoramic Imaging Project: Electronic Document, available at http://www.xrez.com/yose_proj/Yose_result.html